Tailoring Thermotropic Liquid Crystalline Properties of Random Copolymers Based on Vinyl Monomers with Laterally Attached Mesogenic and Nonmesogenic Substituents via No Spacer

Hui Tang, Zhiguo Zhu, Xinhua Wan,* Xiaofang Chen, and Qifeng Zhou*

Beijing National Laboratory for Molecular Sciences, Key Laboratory of Polymer Chemistry and Physics of Ministry of Education, College of Chemistry and Molecular Engineering, Peking University, Beijing 100871, China

Received April 19, 2006; Revised Manuscript Received July 27, 2006

ABSTRACT: Vinyl copolymers comprising mesogenic 2,5-bis[(4-methoxyphenyl)oxycarbonyl]styrene (MPCS) and nonmesogenic 2,5-di(*n*-butoxycarbonyl)styrene (BCS) were synthesized via free radical polymerization. The random nature of the copolymers was characterized by the single glass transition and the reactivity ratios of the comonomers ($r_{MPCS} = 1.51$, $r_{BCS} = 0.42$ by ^{1}H NMR). In contrast to the copolymers based on MPCS and other nonmesogenic monomers such as styrene (St) and methyl methacrylate (MMA), which display no mesophase when the content of St or MMA exceeds a certain amount, all the copolymers obtained in this study showed quite stable liquid crystalline properties regardless of the copolymer compositions. A combination of differential scanning calorimetry, polarized light optical microscopy, and one-dimensional and two-dimensional wide-angle X-ray diffraction analyses demonstrated that the liquid crystalline phase structures of this series of copolymers were strongly composition dependent. When the molar fraction of MPCS in feed (M_{MPCS}) was above 0.5, a hexatic columnar nematic (Φ_{HN}^{I}) phase was formed with a constant *d* spacing value of 1.58 nm. When M_{MPCS} was below 0.1, a hexagonal columnar (Φ_H) phase was observed, and the corresponding *d* spacing was about 1.44 nm. In between $0.1 < M_{MPCS} < 0.5$, another hexatic columnar nematic (Φ_{HN}^{II}) phase could be recognized with tunable *d* spacing relying on the copolymer compositions.

Introduction

Since first reported by Hessel and Finkelmann in 1985, "side-on fixed" liquid crystalline polymers (LCPs) have constituted a novel class of side-chain liquid crystalline polymers (SCLCPs) and have attracted enormous attention because of the fascinating challenges they offer in understanding the influence of the macromolecular structure on the liquid crystalline behavior.[1−5] In these macromolecules, the mesogenic groups are attached to the backbone at the waist position or mass center instead of at the end position as in conventional SCLCPs ("side-end fixed").

SCLCPs exhibit unusual properties as a consequence of compromise between the orientational ordering, imposed by their mesomorphic character, and the nature to maximal entropy common to all chain systems.[6] For "side-end fixed" LCPs, small-angle neuron scattering (SANS) studies have reveled that the polymer backbones exhibit a strong oblate conformational anisotropy due to the packing between layers in smectic phase and various oblate or prolate conformations in nematic phase depending on temperature or chemical structures of SCLCPs.[6−10] For "side-on fixed" LCPs, however, the polymer main chain usually takes extended global conformation (prolate) on the direction of mesogenic groups since the laterally attached mesogens exert an enhanced "jacket effect" compared to that in conventional "side-end fixed" SCLCPs.[11] Hardouin and co-workers have systematically examined the influence of the length of flexible spacer and aliphatic extremity and the dilution of the mesogenic content in a copolymeric homologous on the propolate anisotropy of the polymer backbone by SANS.[12,13] It was found that short flexible spacer and aliphatic tail and high mesogenic content favor the mesogen/backbone coupling and large conformational anisotropy of the main chain. Most laterally attached SCLCPs display nematic mesophase (N) although smectic A (S_A) and smectic C (S_C) phases have also been demonstrated in some cases with well-designed structures.[1−5,14−22] The type of mesogen and the length of flexible spacer linking the backbone and the side groups as well as the terminal substituents are usually believed to be the primary factors determining the phase structures exhibited by a given such polymer, while other properties, such as the nature of the polymer backbone, configuration, and polydispersity, are considered as the secondary factors in tuning the natural ordering of the side mesogenic units.[23]

An extreme form of "side-on fixed" LCPs is mesogen-jacketed liquid crystalline polymers (MJLCPs), in which the rodlike mesogens are connected to every other carbon atom of polymer main chain at the waist position or mass center via a single covalent bond.[4,24−38] The direct linking to the chain makes the interaction between rigid and bulky side groups and polymer backbone so strong that side chains and main chain can act as a whole to achieve mesophase; i.e., the mesogenic units are coincided with the macromolecules themselves. In contrast to MJLCPs, it is usually not possible to provide any mesomorphic property via direct linking mesogens to the backbone, with only a few exceptions,[39] even in the case of conventional "side-end fixed" LCPs. A number of MJLCPs, such as poly(2-vinyl-hydroquinone ester) (PVHQE),[27,28,37,38] poly(2-vinyl-1,4-phenylenediamide) (PVPDA),[35] poly(2-vinylterephthalate ester) (PVTAE),[24−26,29−31,33,34,36] and poly(2-vinyl-*p*-terphenyl ether) (PVTPE),[32] with different side mesogens have been synthesized to tailor and optimize liquid crystallinities.

Poly{2,5-bis[(4-methoxyphenyl)oxycarbonyl]styrene} (PMPCS) is among the most extensively studied MJLCPs.[33] Its monomer,

* Corresponding authors. Xinhua Wan: 86-10-62754187 (Tel), 86-10-62754187 (Fax), xhwan@pku.edu.cn (e-mail). Qifeng Zhou: 86-10-62756660 (Tel), 86-10-62751708 (Fax), qfzhou@pku.edu.cn (e-mail).

10.1021/ma0608774 CCC: $33.50
Published on Web 09/06/2006

2,5-bis[(4-methoxyphenyl)oxycarbonyl]styrene (MPCS), melts into nematic phase at 109 °C and enters isotropic phase at 144 °C. The phase transition and structure of PMPCS are closely related to the molar mass of the polymer.[29] With an increase in molecular weight, amorphous, columnar nematic (Φ_N), and hexatic columnar nematic (Φ_{HN}) phase are observed. The mesophase appears almost immediately above the glass transition and does not vanish on the subsequent heating or cooling process. It is believed that the liquid crystalline phase is formed by the cooperation of the backbone together with the laterally attached mesogenic units to construct cylinders, which act as the building blocks of the mesophase. Poly[2,5-di(*n*-butoxycarbonyl)styrene] (PBCS) is another interesting MJLCPs type LCP, which is prepared from the nonmesogenic monomer, 2,5-di(*n*-butoxycarbonyl)styrene (BCS), via free radical polymerization. PBCS is similar to PMPCS in the way that side groups are linked laterally to the main chain through no spacer. Although no conventional rodlike mesogen presents in the molecule, it forms two-dimensional hexagonal columnar (Φ_H) phase at temperatures much higher than its glass transition as characterized by higher orders of one- and two-dimensional wide-angle X-ray diffractions.[31,40]

Copolymerization represents one of the simplest synthetic techniques to manipulate the phase transitions of both main-chain and side-chain liquid crystalline polymers and to widen their application range as high-performance materials.[39,41−44] Varying the nature and molar ratio of comonomers, it is possible to exert effective control over the transition temperature and, to some extent, the phase structure.[45−58] For MJLCPs, however, the incorporation of non-liquid-crystalline monomer in the polymer chain would disturb the self-assembly of the macromolecule as a whole to form mesophase. For example, when MPCS is copolymerized with non-liquid-crystalline vinyl monomers, such as styrene (St) and methyl methacrylate (MMA), mesophase can only be observed when the molar contents of MPCS in copolymers exceed about 89 and 84%, respectively.[59] Similar phenomena have also been observed in some linear flexible liquid crystalline polymers without typical mesogenic building blocks such as polydialkylsilylenes and polyphosphazenes.[60−62] It is speculated that the constitutional disorder, which dilutes the concentration of mesogenic units and disrupts the interactions between backbone and side groups, is responsible for the destabilization of the mesophase.[63,64]

This article presents the mediation of the liquid crystalline properties of the random copolymers based on MPCS and BCS. Although BCS cannot form mesophase by itself as St and MMA, when it is radically copolymerized with MPCS, all the resultant copolymers display stable mesophases above their glass transition temperatures regardless of the amount of MPCS incorporated into. The liquid crystalline behaviors of this series of copolymers are thoroughly investigated to clarify the effect of structural disorder on the liquid crystallinity of copolymers using WAXD experiments. By tuning the molar content of MPCS in feed, variation of both liquid crystalline phase structure and the mesophase dimension of the copolymers is achieved. This study provides a unique example of tuning the liquid crystalline properties of MJLCPs by random copolymerization with non-mesogenic monomer within the whole composition range.

Experimental Section

Materials. The two monomers MPCS and BCS were synthesized according to the procedures reported previously.[30,33] 2,2′-Azobis(isobutyronitrile) (AIBN, Beijing Chemical Co., 95%) was purified by recrystallization from ethanol before use. Chlorobenzene (Beijing Chemical Co., A.R.) used as the polymerization solvent was washed successively with concentrated sulfuric acid (Beijing Chemical Co., 98%), aqueous solution of $NaHCO_3$ (Beijing Chemical Co., A.R.), and deionized water and distilled out from calcium hydride (Beijing Chemical Co., A.R.) under an argon atmosphere. Tetrahydrofuran (THF, Beijing Chemical Co., A.R.) and methanol (Beijing Chemical Co., A.R.) employed in dissolving and precipitating polymers were used as purchased. THF (Aldrich, gas chromatography grade) were directly used in the size exclusion chromatography (SEC) and UV−vis absorption spectra. Unless otherwise specified, all other solvents and reagents were purchased from Beijing Chemical Co. and used as received.

Copolymerization. Copolymerization was carried out in solution. In a typical run, MPCS (0.22 g, 0.56 mmol), BCS (1.5 g, 5.0 mmol), AIBN (0.45 mg, 2.8×10^{-3} mmol), and chlorobenzene (7.0 g, 63 mmol) were successively introduced into a reaction tube. After three freeze−pump−thaw cycles, the tube was sealed under vacuum and inserted into a thermostated oil bath at 60 °C. The polymerization was allowed to continue for 2 h. After the polymerization was terminated by breaking the tube, the reactant was diluted with 10 mL of THF and then precipitated in 200 mL of methanol. The dissolution in THF and precipitation in methanol were repeated three times to eliminate the unreacted monomers completely. The copolymers were dried at 60 °C under vacuum for 24 h before further characterizations were performed. The monomer conversion in weight was 5.6%. The number-average molecular weight and polydispersity of the resultant copolymer were 1.82×10^5 and 1.71, respectively. ^{1}H NMR (δ, ppm, acetone-d_6): 0.6−2.0 (broad peaks, $-CH_2CH$ protons in the backbone and $-CH_2CH_2CH_3$ protons in the side groups of BCS), 3.2−4.5 (broad peaks, $-OCH_3$ protons in MPCS and $-OCH_2$ protons in BCS), 6.2−7.0 (broad peaks, side phenyl ring protons of MPCS), and 7.1−8.0 (broad peaks, middle phenyl ring protons of MPCS and phenyl ring protons of BCS).

Instruments and Measurements. The number-average molecular weights (M_n), weight-average molecular weights (M_w), and polydispersity distribution index (PDI, M_w/M_n) of the resultant copolymers were estimated by a size exclusion chromatography (SEC) instrument with a Waters 2410 refractive index detector. Three Waters Styragel columns with 10 μm bead size were connected in series. Their effective molecular weight ranges were 100−10000 for Styragel HT2, 500−30000 for Styragel HT3, and 5000−600000 for Styragel HT4. The pore sizes were 50, 100, and 1000 nm for Styragel HT2, HT3, and HT4, respectively. THF was employed as the eluant at a flow rate of 1.0 mL min^{-1} at 35 °C, and the calibration curve was obtained with monodispersed polystyrenes as standards. All the announced molecular weights in this paper were in equivalent of standard polystyrenes. ^{1}H NMR spectra were recorded on a Bruker ARX 400 MHz spectrometer with acetone-d_6 as solvent and TMS as an internal reference. UV−vis absorption spectra were performed on a Shimadzu UV-2101PC spectrophotometer with THF as solvent at room temperature.

The thermal transitions of copolymers were investigated by using differential scanning calorimetry (DSC) on a TA Q100 calorimeter in a temperature range of −90 to 200 °C at a heating rate of 40 °C min^{-1} under continuous nitrogen flow. All the data were based on the second heating process after cooling at 2 °C min^{-1} from 200 °C. *n*-Octane (mp 56.76 °C) and indium (mp 156.78 °C) were used to calibrate the instrument. The average sample mass was about 2 mg, and the nitrogen flow rate was 50 mL min^{-1}. A TA Q600 instrument was used for thermogravimetric analysis of the copolymers. Generally, about 3 mg of sample was heated from 30 to 600 °C at a heating rate of 20 °C min^{-1} under nitrogen flow.

One-dimensional (1D) WAXD powder experiments were performed on a Philips X'Pert Pro diffractometer with a 3 kW ceramic tube as the X-ray source (Cu Kα radiation) and an X'celerator detector. A temperature control unit in conjunction with a diffractometer was utilized to study the structure evolutions as a function of temperature changing at constant heating and cooling rates. Films with thickness of ~1 mm were mounted on copper sheets, and the diffraction patterns were collected by reflection mode. Background scattering pattern was recorded and subtracted from the WAXD patterns of samples.

Scheme 1. Synthesis and Chemical Structures of Copolymers Comprising 2,5-Bis[(4-methoxyphenyl)oxycarbonyl]styrene (MPCS) and 2,5-Di(*n*-butoxycarbonyl)styrene (BCS)[a]

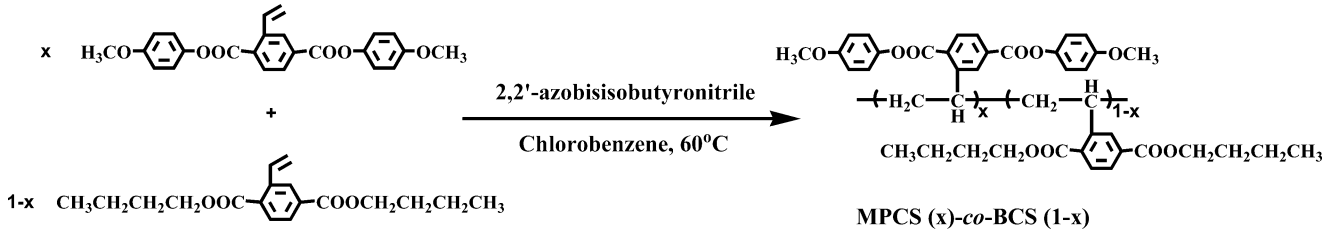

[a] The numbers in the parentheses indicate the molar fraction of each monomer in feed.

Table 1. Copolymerization Results of 2,5-Bis[(4-methoxyphenyl)oxycarbonyl]styrene (MPCS) with 2,5-Di(*n*-butoxycarbonyl)styrene (BCS)

sample[a]	conv (%)	M_n ($\times 10^5$)[b]	PDI[b]	T_g(°C)[c]	liquid crystallinity[d]
MPCS(0.93)-*co*-BCS(0.07)	8.8	3.68	1.57	119.0	yes
MPCS(0.86)-*co*-BCS(0.14)	5.9	2.96	1.25	112.4	yes
MPCS(0.80)-*co*-BCS(0.20)	10.4	2.66	1.39	105.4	yes
MPCS(0.67)-*co*-BCS(0.33)	9.2	3.28	1.23	100.5	yes
MPCS(0.58)-*co*-BCS(0.42)	8.1	2.12	1.62	96.9	yes
MPCS(0.50)-*co*-BCS(0.50)	7.2	1.58	1.92	81.0	yes
MPCS(0.40)-*co*-BCS(0.60)	5.2	1.66	1.86	78.7	yes
MPCS(0.30)-*co*-BCS(0.70)	8.6	2.99	1.72	66.1	yes
MPCS(0.21)-*co*-BCS(0.79)	6.3	1.86	1.61	47.6	yes
MPCS(0.15)-*co*-BCS(0.85)	9.7	2.85	1.69	38.2	yes
MPCS(0.10)-*co*-BCS(0.90)	5.6	1.82	1.71	28.6	yes
MPCS(0.05)-*co*-BCS(0.95)	10.1	3.69	1.88	18.9	yes

[a] Polymerization condition: chlorobenzene solution (20 wt %); temperature: 60 ± 0.5 °C; initiator: 2,2′-azobis(isobutyronitrile) (AIBN) (0.05%, based on total mole number of monomers). The numbers in the parentheses indicate the molar fraction of each monomer in feed. The abbreviations of the copolymers are the same in Table 2. [b] M_n: number-average molecular weight; M_w: weight-average molecular weight; PDI: polydispersity distribution index (M_w/M_n). Obtained from size exclusion chromatography, monodispersed polystyrenes as standards. [c] T_g: glass transition temperature. Obtained from the second heating differential scanning calorimetry experiments. [d] Determined by polarized light optical microscope observations.

Two-dimensional (2D) WAXD fiber patterns were obtained using a Bruker D8 Discover diffractometer with GADDS (general area detector diffraction system) as a detector. The two-dimensional diffraction patterns were recorded in transmission mode at room temperature. Fibers were drawn with stretching at a rate of about 1 m s^{-1} at 180 °C and quenched to room temperature for test. Background scattering pattern was recorded and subtracted from the WAXD patterns of samples.

Phase morphology was identified via a Leica DML polarized light optical microscope (POM) with Mettler hot stage (FP 82 HT with a FP-90 central processor). The sample films were prepared by the solution-cast method, and the thicknesses were kept at several microns.

Results and Discussion

Copolymerization. Copolymerizations of MPCS with BCS were carried out in chlorobenzene at 60 °C using AIBN as the initiator (Scheme 1). A series of copolymers, MPCS(x)-*co*-BCS-($1 - x$), were obtained. The numbers in the parentheses following the abbreviation of each monomer indicated their molar fractions in feed. To minimize the effect of unequal monomer consumption during the process of copolymerization, the monomer conversions were kept below 10% in most experiments.[65] The copolymerization results of MPCS with BCS are summarized in Table 1 with the molar percentage of MPCS in feed ranging from 0.93 to 0.05. All the copolymers obtained had relatively high molecular weights and narrow molecular weight distributions (PDI < 2.0).

Compositions. The chemical compositions of the resultant copolymers were first estimated from ^{1}H NMR spectra with acetone-d_6 as solvent. Figure 1 presents ^{1}H NMR spectra of a representive copolymer, MPCS(0.10)-*co*-BCS(0.90), and the two corresponding homopolymers, PMPCS and PBCS. The assignment of each peak can be seen from the figure. The partial molar proportions of the two monomers in the copolymers (m_{MPCS} and m_{BCS}) were calculated according to

$$(6m_{MPCS} + 4m_{BCS})/(11m_{MPCS} + 3m_{BCS}) = I_{alkoxy}/I_{aromatic} \quad (1)$$

where I_{alkoxy} and $I_{aromatic}$ are defined as relative intensities of CH_3O- and $-CH_2O-$ groups and aromatic groups, respectively.

Since the monomer ratios in copolymers were the key parameters influencing the liquid crystallinities of copolymers, UV−vis absorption spectra were also used to verify the results of ^{1}H NMR spectra.

For a binary system in the solution, the Beer−Lambert law states

$$A = \epsilon_1 bc_1 + \epsilon_2 bc_2 \quad (2)$$

where A is the absorbance, b is the cell length in centimeter, and c_1, c_2 and ϵ_1, ϵ_2 are the molar concentrations and the molar absorptivities of the solutes, respectively.

Measuring the absorbance of a series of standard solutions containing different ratios of analytes, the molar concentrations of which are known, and plotting the molar absorptivity against the ratio of the analytes gives a straight line. From the slope and intercept, ϵ_1 and ϵ_2 can be calculated. On the other hand, given the molar absorptivity of a system containing two known analytes, the ratio of the analytes is available.

UV−vis absorption spectra were recorded in THF at room temperature. The molar absorptivities of MPCS and BCS homopolymers at 270 nm were calculated as $\epsilon_{PMPCS} = 8.22 \times 10^3$ and $\epsilon_{PBCS} = 1.70 \times 10^3$. The molar absorptivity vs MPCS molar fraction in PMPCS/PBCS blends is shown in Figure 2, and the respective molar absorptivity is figured out as $\epsilon_{PMPCS} = 8.23 \times 10^3$ and $\epsilon_{PBCS} = 1.66 \times 10^3$, which agreed well with those from corresponding homopolymers. Therefore, m_{MPCS} and m_{BCS} were calculated by the plots of Figure 2 with assumption that the absorptions of chromophores at 270 nm had not changed significantly after copolymerization when compared with the corresponding homopolymers. The results are listed in Table 2.

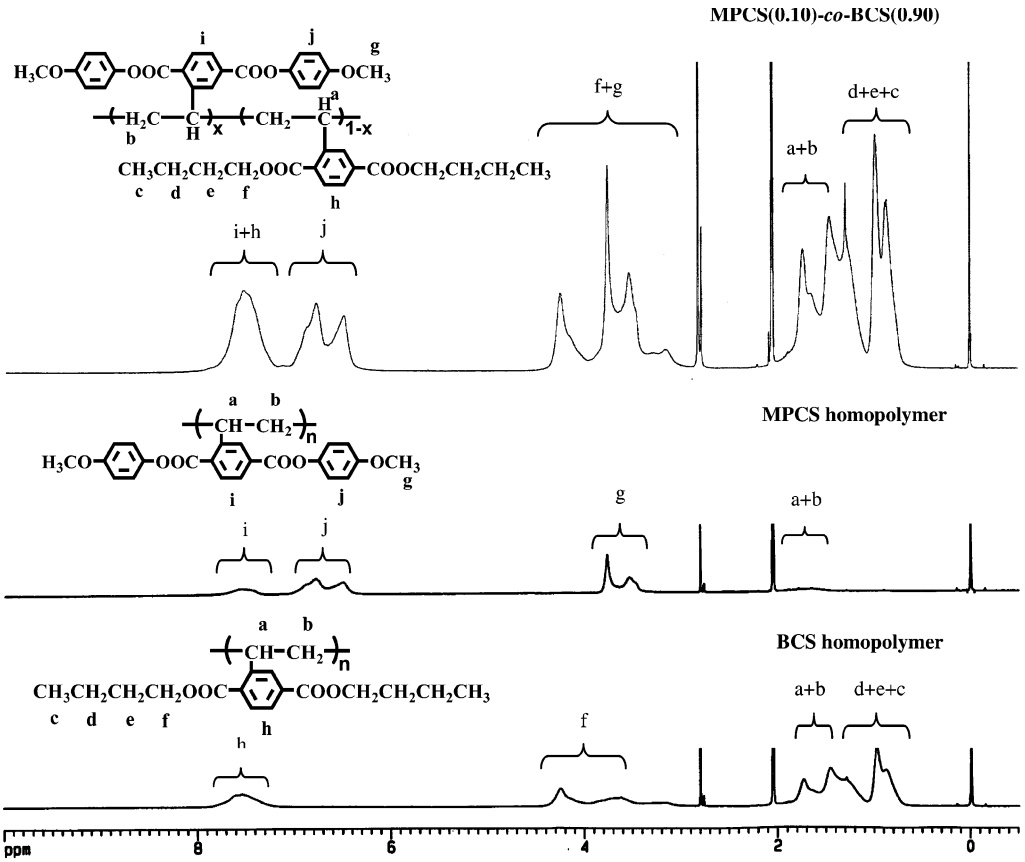

Figure 1. ^{1}H NMR spectra of a representive copolymer (molar fraction of MPCS in feed is 0.10), MPCS homopolymer, and BCS homopolymer (acetone-d_6, 400 MHz).

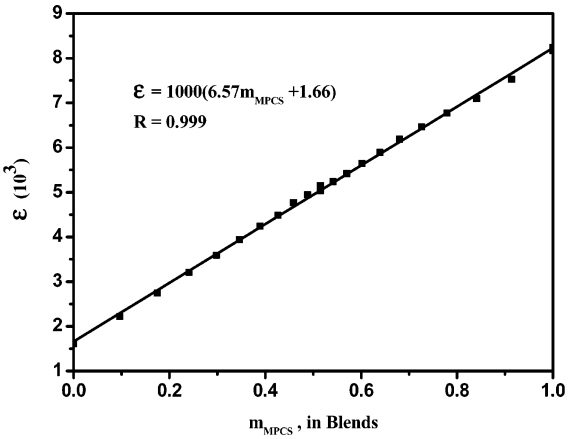

Figure 2. Molar absorptivity (ϵ) in blends of MPCS and BCS homopolymers vs MPCS molar fraction (m_{MPCS}).

Reactivity Ratio. To examine the structural parameters of copolymers and the effects of monomer composition on liquid crystallinity, reactivity ratios were characterized from the monomer ratios in feed and the copolymer compositions using the extended Kelen−Tudos (EKT) linearization method with consideration of monomer conversions.[65−71]

In the EKT method, X and Y are defined as F_1/F_2 and f_1/f_2, respectively, with F_1, F_2, f_1, f_2 being the molar fractions of monomer in feed and in copolymer. The partial molar conversions for the two monomers (ζ_1 and ζ_2) are defined as

$$\zeta_1 = \zeta_2(Y/X) \tag{3}$$

$$\zeta_2 = W(\mu + X)/(\mu + Y) \tag{4}$$

where μ is the ratio of molecular weights of monomer 2 to that of monomer 1 and W is the weight conversion of copolymerization.

Then

$$Z = \log(1 - \zeta_1)/\log(1 - \zeta_2) \tag{5}$$

with Z factor, a linearized version of the copolymer equation is defined in the EKT linearization method:

$$\eta = (r_1 + r_2/\alpha)\,\xi - r_2/\alpha \tag{6}$$

η and ξ are equal to $G/(\alpha + H)$ and $H/(\alpha + H)$, respectively, where G and H are defined as $(Y - 1)/Z$ and Y/Z^2, respectively. The α parameter [$\alpha = (H_M H_m)^{1/2}$] is a constant used to equally distribute the x-axis values in a range of 0 to 1 with the maximum (M) and minimum (m) values of H.

Plots of η and ξ for the EKT method can be prepared for estimating r_1 and r_2 which represent the reactivity ratios of monomer 1 and monomer 2.

Figure 3 presents the EKT plots of MPCS(x)-*co*-BCS($1 - x$) based on ^{1}H NMR and UV−vis spectra results, respectively. The reactivity ratios of MPCS and BCS (r_{MPCS} and r_{BCS}) together with the copolymer compositions are depicted in Table 2. Although the results from ^{1}H NMR and UV−vis spectra are not quite identical, the values of $r_{MPCS}r_{BCS}$ are close to 1, which is typical for random copolymerization, indicating that no significant heterogeneity existed and the monomer units in the polymer chain had a tendency of random distribution.[72]

Both MPCS and BCS can be considered as substituted styrene monomers. The substituent of the former is much larger and more rigid than that of the latter. However, as suggested by reactivity ratios, $r_{MPCS} > 1 > r_{BCS}$, MPCS was more reactive

Table 2. Compositions of Copolymers and Reactivity Ratios of MPCS and BCS Based on ^{1}H NMR and UV−Vis Absorption Spectra

sample	$m_{MPCS-NMR}$ [a]	^{1}H NMR spectra	$m_{MPCS-UV}$ [b]	UV−vis spectra
MPCS(0.93)-*co*-BCS(0.07)	0.95		0.97	
MPCS(0.86)-*co*-BCS(0.14)	0.89		0.94	
MPCS(0.80)-*co*-BCS(0.20)	0.86		0.91	
MPCS(0.67)-*co*-BCS(0.33)	0.79		0.82	
MPCS(0.58)-*co*-BCS(0.42)	0.72		0.76	
MPCS(0.50)-*co*-BCS(0.50)	0.65	r_{MPCS} [c] = 1.51	0.68	r_{MPCS} = 2.49
MPCS(0.40)-*co*-BCS(0.60)	0.54	r_{BCS} [c] = 0.42	0.58	r_{BCS} = 0.44
MPCS(0.30)-*co*-BCS(0.70)	0.44	$r_{MPCS}r_{BCS}$ = 0.63	0.49	$r_{MPCS}r_{BCS}$ = 1.10
MPCS(0.21)-*co*-BCS(0.79)	0.35		0.37	
MPCS(0.15)-*co*-BCS(0.85)	0.26		0.29	
MPCS(0.10)-*co*-BCS(0.90)	0.16		0.21	
MPCS(0.05)-*co*-BCS(0.95)	0.10		0.11	

[a] $m_{MPCS-NMR}$: molar fraction of MPCS in copolymer obtained from ^{1}H NMR spectra. [b] $m_{MPCS-UV}$: molar fraction of MPCS in copolymer obtained from UV−vis absorption spectra. [c] r_{MPCS} and r_{BCS}: reactivity ratios of MPCS and BCS, respectively.

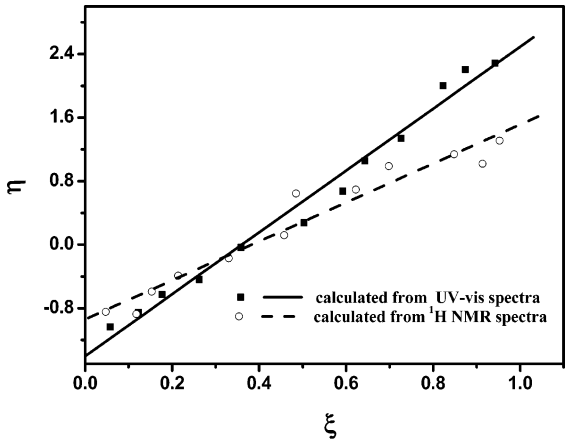

Figure 3. Extended Kelen−Tudos (EKT) method plots determined by ^{1}H NMR and UV−vis absorption spectra. η and ξ are defined as described in the text.

than BCS. Ober and co-workers noticed the similar behavior in nitroxide-mediated free radical polymerization of 2,5-bis[(4-butylbenzoyl)oxy]styrene (BBOS), a similar mesogenic monomer to MPCS.[73] BBOS polymerized much faster than its nonmesogenic model, 2,5-diacetoxystyrene in bulk, whereas in a dilute solution, the polymerization rates of both monomer were comparable. The increased reactivity of BBOS in the bulk was attributed to the presence of a nematic phase that could lead to localized ordering of the monomers. Although MPCS is able to form a nematic phase in melt, the fact that MPCS has larger reactivity than BCS cannot be interpreted by localized lining up of the monomer because the copolymerization is carried out in an isotropic solution. One possible reason is that the large substituents in MPCS impart a remarkable steric hindrance and enhance the stability of the MPCS radicals at chain ends, while as a rule copolymerization tends to form more stable radicals. However, it should be figured out that there are a lot to be done before a valid explanation can be made. A detailed investigation into the mechanism to activate MPCS has been underway.

Thermal Behavior. The dependence of the thermal transition temperatures on the compositions of MPCS(x)-*co*-BCS($1 - x$) copolymers was studied by DSC experiments. Since fast heating of slowly cooled samples induces endothermic hysteresis peaks in glass transition region and glass transition can be more evident,[74] a fast heating rate of 40 °C min^{-1} was employed to scan the annealed copolymers, which were prepared by being slowly cooled (2 °C min^{-1}) from 200 °C. The DSC curves were featureless except for glass transitions. For all the copolymers we studied, only single glass transition was identified (Figure 4a), indicating the monomers were placed randomly along the main chain and no phase separation occurred. This was consistent with the results obtained from monomer reactivity ratio study. In comparison, the blends of PMPCS and PBCS (molar ratio = 52:48) displayed two glass transitions as shown in Figure 4b. The glass transition temperature (T_g) of the copolymers increased with the MPCS fraction in feed. This continuous adjustment in T_g was another evidence of molecular-level homogeneity of monomer distribution in the polymer main chain.[74]

Liquid crystalline phases of the copolymers were first studied by POM observation. Since the liquid crystalline properties of both PMPCS and PBCS are molecular weight dependent and the mesomorphic behaviors are almost invariable when the molecular weights are high enough,[29,31] for simplicity, all the copolymers studied here have molecular weights much higher than the critical values for the two homopolymers to form mesophase, and as a result, the molecular weight effect can be ignored. Figure 5 shows the representative images of the textures of MPCS(0.40)-*co*-BCS(0.60) (a) and MPCS(0.10)-*co*-BCS-(0.90) (b) taken at 180 °C. Both PMPCS and PBCS are thermotropic liquid crystalline polymers. PMPCS exhibits star-shaped texture with two or four brushes or schlieren texture,[35] while focal-conic fan texture is the typical image for PBCS.[30] Most of the copolymers studied here showed schlieren and star-shaped textures, implying the formation of nematic mesophase. However, when M_{MPCS} was below 0.1, a focal-conic fan texture similar to BCS homopolymer was displayed.

1D Wide-Angle X-ray Diffraction. To examine the ordered structures developed in these copolymers, 1D WAXD experiments were carried out with the as-cast samples. The mesophase structure of MPCS(x)-*co*-BCS($1 - x$) was found to rely strongly on the comonomer fraction. Figure 6 illustrates the temperature variable 1D WAXD patterns of MPCS(0.10)-*co*-BCS(0.90) in the low 2θ angle (between 2.5° and 9.5°) region, which were recorded during the first heating and the subsequent cooling runs, respectively. The glass transition temperature of the copolymer was 28.6 °C. When the temperature was above 28.6 but below 130 °C, a scattering halo was observed. At higher temperatures, the scattering halo became asymmetric and could be deconvoluted into one broad halo and a narrow reflection peak which centered at $2\theta = 5.9°$ (d spacing of 1.50 nm) and 6.2° (d spacing of 1.42 nm) separately (the dashed curves in Figure 6a). A Gaussian function was used to precisely identify the positions of the scattering halo and reflection peak. Raising temperature (below 190 °C) led to a substantial enhancement of the reflection peak intensity, and the peak shifted continuously and slightly to lower 2θ angle due to the thermal expansion. When the temperature was higher than 190 °C, the mesophase formed seemed to become less ordered since the intensity of the narrow reflection peak began to decrease. However, the

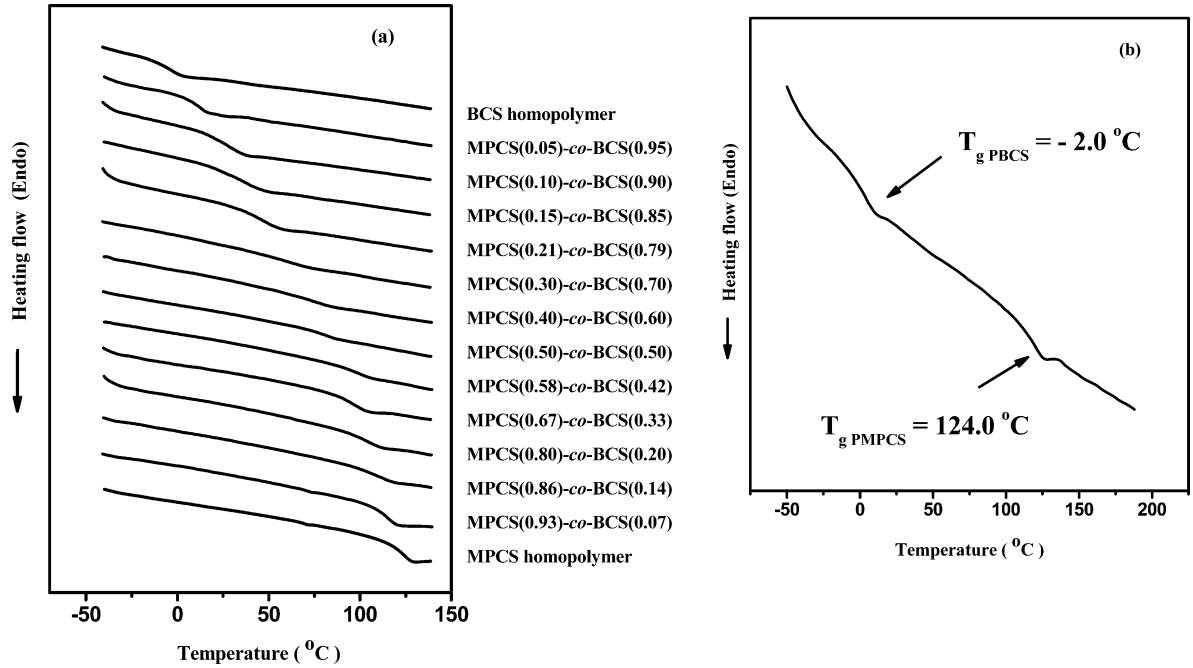

Figure 4. Sets of differential scanning calorimetry curves of copolymers comprising MPCS and BCS during the second heating process at a heating rate of 40 °C min^{-1} after cooling at 2 °C min^{-1} (a) and the thermogram of the blend of MPCS and BCS homopolymers (molar ratio of MPCS is 0.52) (b). T_{gPMPCS} and T_{gPBCS} are the glass transition temperatures of MPCS and BCS homopolymers in blend, respectively.

reflection peak remained apparent until the highest temperature we studied, i.e., 250 °C. The copolymer was quite thermal stable, and the 1% weight loss temperature was higher than 300 °C. Therefore, the observed reduction in the reflection intensity could not be attributed to the thermal decomposition, but an isotropization transition was indicated. When cooled slowly from 250 °C, the strongest reflection peak appeared again at 190 °C, which agreed well with the heating process. The intensity of reflection peak decreased with lowering temperature further. However, the narrow reflection peak still existed even when the sample was cooled to room temperature. It indicated that the mesophase formed at higher temperature could be kept upon cooling although it was less ordered.

In the study of SCLCPs with mesogens terminally attached, it was found that the width of isotropization transition increased when mesogen density decreased. Percec et al. attributed the phenomenon of isotropization transition widening to dissolution of a fraction of the mesogenic units into the polymer backbone layer.[75] As to MPCS(0.10)-*co*-BCS(0.90), since no such kind of microphase separation occurred, the structural irregularity of the copolymer was considered to be the main reason to destabilize the mesophase.

1D WAXD experiments of other copolymers were also performed, and similar phenomena to MPCS(0.10)-*co*-BCS-(0.90) were observed. Figure 7 depicts the *d* spacings measured from sets of 1D WAXD patterns of the copolymers and the corresponding homopolymers at 180 °C as a function of MPCS fractions in feed. Three regions could be identified in terms of the dependence of *d* spacing, which ranged from 1.58 to 1.44 nm, on the copolymer composition. When M_{MPCS} was above 0.5, the copolymers had a same value of *d* spacing (1.58 nm) as that of PMPCS, corresponding to the narrow reflection peak at low angle ($2\theta = 5.6°$). When M_{MPCS} was below 0.1 (including 0.1), the copolymers showed another constant *d* spacing (1.44 nm, $2\theta = 6.1°$), which was the same as that of PBCS. In between $0.10 < M_{MPCS} < 0.50$, the *d* spacing changed from 1.50 to 1.57 nm. The results demonstrated that by tuning the comonomer fraction in feed the mesophase dimension of MPCS-(*x*)-*co*-BCS($1 - x$) copolymers could be controlled effectively. From 1D WAXD experiments alone, however, it was difficult to distinguish the mesophase structures of the copolymers. Therefore, 2D WAXD experiments were carried out and discussed in detail in the following section.

2D Wide-Angle X-ray Diffraction. 2D WAXD experiments on the oriented samples are essential and important in identification of polymer structures. With this technique, Yin et al. have studied the mesophase of BCS homopolymer. Although BCS is not able to self-organize into an ordered phase in melt state, the polymer from it does have stable liquid crystallinity.[30] It is believed that the building blocks involve entire molecules taking relatively extended conformations. Recently, a detailed investigation on the phase structure of MPCS homopolymers has been reported by Ye et al.[29] They found that a hexagonal lateral packing of the cylinders existed in the polymer when the molecular weight was higher than 1.6×10^4. However, this hexagonal lateral packing lacked long-range order and was named as the Φ_{HN} phase. When the molecular weight was lower than 1.6×10^4 but higher than 1.0×10^4, a Φ_N phase was formed. The mesophases of MPCS(*x*)-*co*-BCS($1 - x$) were studied by utilizing a similar method in this study.

Figure 8a shows the 2D WAXD pattern of the oriented MPCS(0.50)-*co*-BCS(0.50) with the X-ray incident beam perpendicular to the fiber axis. A pair of strong diffraction arcs could be seen on the meridian at $2\theta = 5.6°$ (*d* spacing of 1.58 nm), indicating that the ordered structure had been developed along the direction perpendicular to the fiber axis on the nanometer scale. Since no higher order diffractions could be identified on the meridian even after a prolonged exposure time, the 2D WAXD pattern with the X-ray incident beam parallel to the fiber axis was recorded and shown in Figure 8b. A 6-fold symmetry of the (100) diffractions at $2\theta = 5.6°$ (*d* spacing of 1.58 nm) existed on the nanometer scale was exhibited. It indicated a hexagonal column lattice structure perpendicular to the fiber axis. The corresponding azimuthal intensity profile which exhibited six maxima with an angle of 60° between two adjacent diffraction maxima is shown in Figure 8c. Therefore,

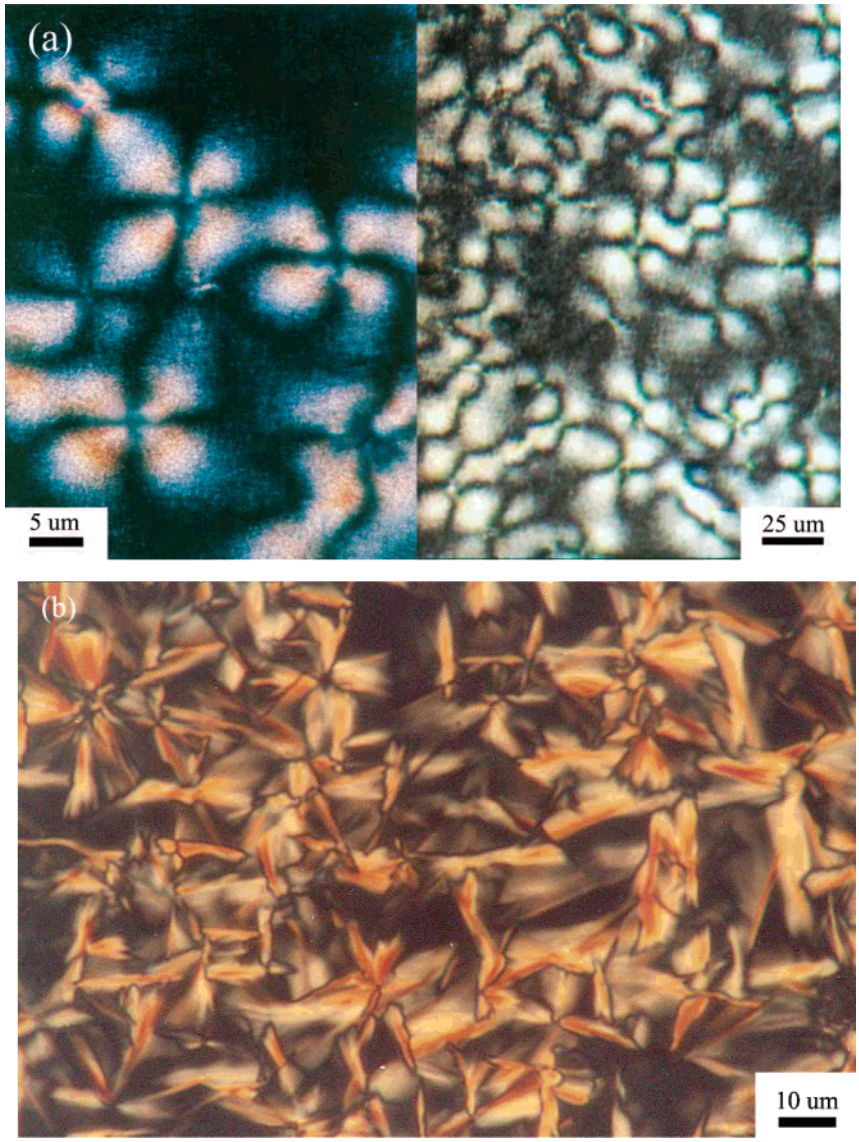

Figure 5. Polarized light optical photographs of the copolymers at 180 °C. The molar fractions of MPCS in feed are 0.40 (a) and 0.10 (b), respectively.

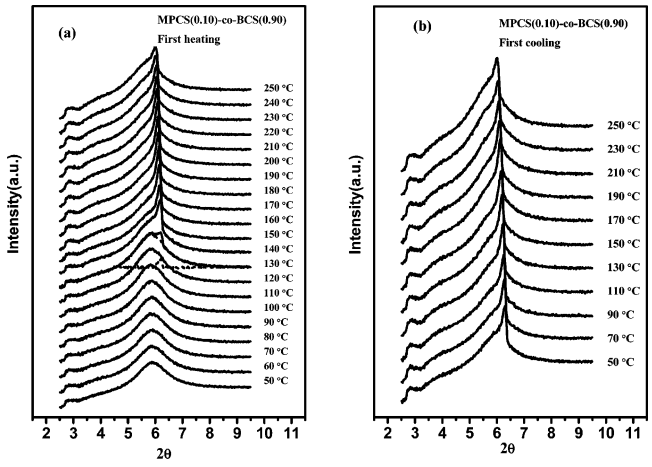

Figure 6. One-dimensional wide-angle X-ray diffraction powder patterns in the low 2θ angle region of the copolymer during the first heating (a) and the subsequent cooling course (b). The molar fraction of MPCS in feed is 0.10.

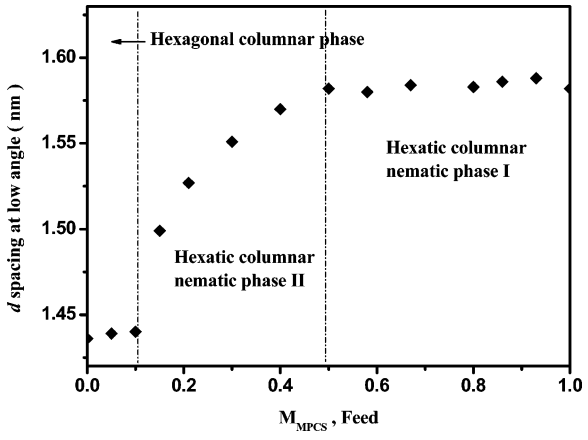

Figure 7. *d* spacing data from one-dimensional wide-angle X-ray diffraction patterns as functions of molar fraction of MPCS in feed (M_{MPCS}) at 180 °C. Three regions are identified which represent as hexatic columnar nematic I (Φ_{HN}^{I}) phase (*d* spacing of 1.58 nm), hexatic columnar nematic II (Φ_{HN}^{II}) phase (*d* spacing from 1.57 to 1.50 nm), and hexagonal columnar (Φ_H) phase (*d* spacing of 1.44 nm).

the liquid crystalline phase should be a Φ_{HN} phase, and a hexagonal lateral packing of the cylinders with each cylinder having an average diameter of 1.82 nm was developed without long-range order perpendicular to the fiber axis. Similar results

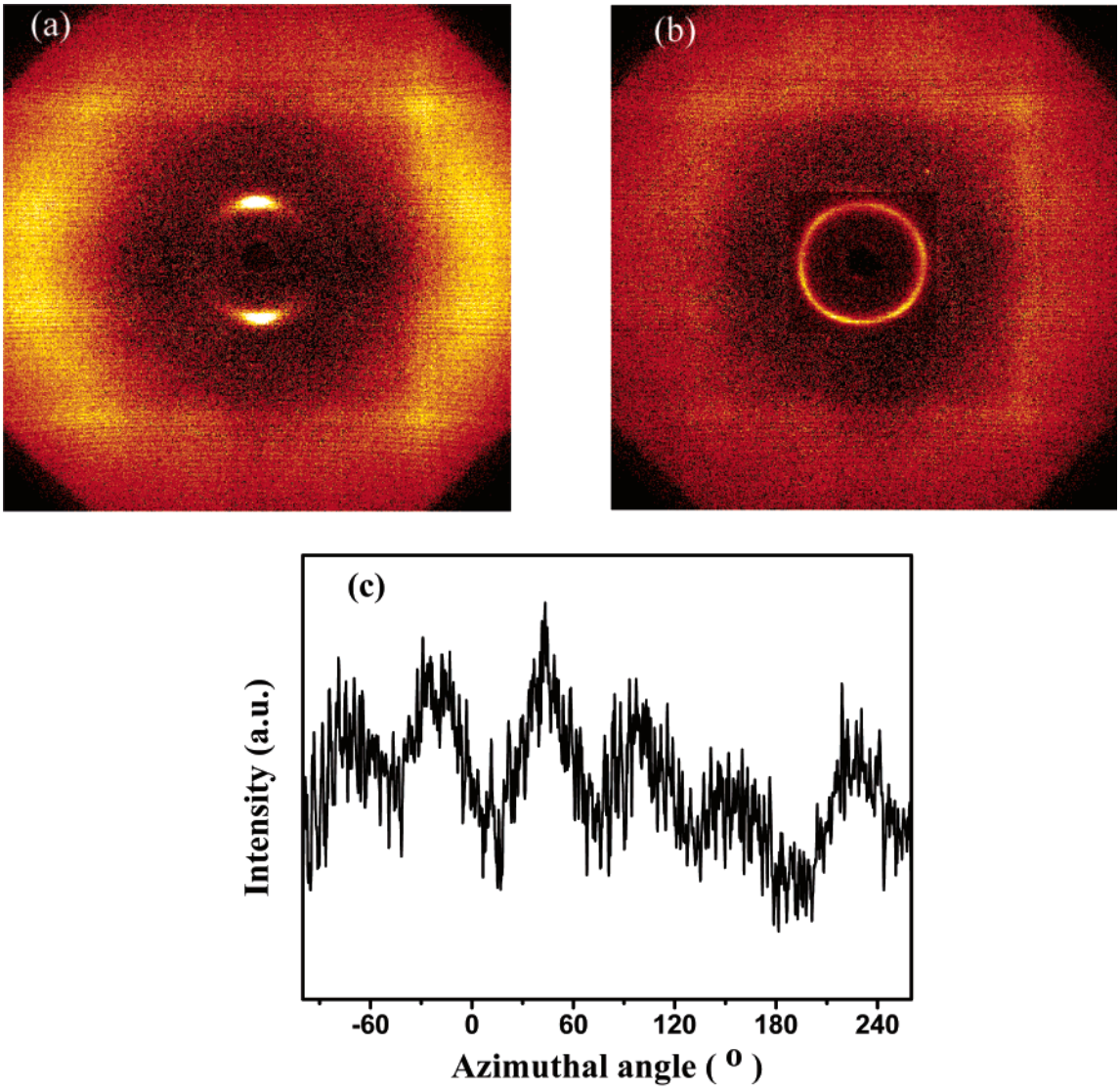

Figure 8. Two-dimensional wide-angle X-ray diffraction fiber patterns of the copolymer in which the molar fraction of MPCS in feed is 0.50. The X-ray incident beam was (a) perpendicular to the fiber axis (the meridian direction), (b) along the meridian direction, and (c) the azimuthal scanning data of the low 2θ angle region diffraction.

were obtained in other copolymers except for MPCS(0.10)-*co*-BCS(0.90) and MPCS(0.05)-*co*-BCS(0.95), indicating that a Φ_{HN} phase existed in these copolymers.

The investigation of ordered structure of MPCS(0.10)-*co*-BCS(0.90) was of particular interest. High orders of the diffractions were identified when the X-ray incident beam was parallel to the fiber axis (Figure 9a). The *d* spacing value of the diffraction arcs at the lowest 2θ angle was 1.44 nm, which was identical to that obtained in 1D WAXD experiment (shown in Figure 9b). Two additional diffraction arcs could also be observed at $2\theta = 10.6°$ (*d* spacing of 0.85 nm) and $2\theta = 12.2°$ (*d* spacing of 0.73 nm). These three scattering vector ratios followed $1:3^{1/2}:4^{1/2}$, and the diffraction arcs could be assigned to be the (100), (110), and (200) plane, respectively, indicating that this mesophase structure possessed a long-range periodic hexagonal packing along the lateral direction perpendicular to the fiber axis. It demonstrated the substantial lateral order of the hexagonal lattices and a hexagonal columnar (Φ_H) phase was achieved in MPCS(0.10)-*co*-BCS(0.90). The average diameter of the corresponding building blocks was about 1.67 nm. Similar results could be achieved in MPCS(0.05)-*co*-BCS-(0.95).

The signal in 2θ around 20° (*d* spacing of $\sim$ 0.43 nm) in Figure 9b was mainly attributed to the short-range ordered structure along the chain axis which indicated the average distance between side groups. In the study of MPCS homopolymers, the *d* spacing at sub-nanometer is about 0.43 nm, and a conclusion that the polymers possess a quite extended main-chain conformation is drawn.[29] In MPCS(*x*)-*co*-BCS($1 - x$) samples here, we speculate that the *d* spacing of nearly 0.43 nm also represents the projection of two repeating units along the chain axis.

On the basis of the above studies, the three regions in Figure 7 could be identified as hexatic columnar nematic I (Φ_{HN}^{I}) phase, hexatic columnar nematic II (Φ_{HN}^{II}) phase, and Φ_H phase. In the first region (Φ_{HN}^{I}), where the MPCS molar fraction in feed was higher than 0.5, the copolymers formed the same ordered structures as that of MPCS homopolymer. The structure dimension was independent of the copolymer composition. In the second region (Φ_{HN}^{II}), the copolymers also developed into hexatic columnar nematic phase upon heating; however, the *d* spacing decreased from 1.57 to 1.50 nm when BCS fraction in feed decreased from 0.40 to 0.15. In the third region (Φ_H), the mesophase structures formed by the copolymers were the same

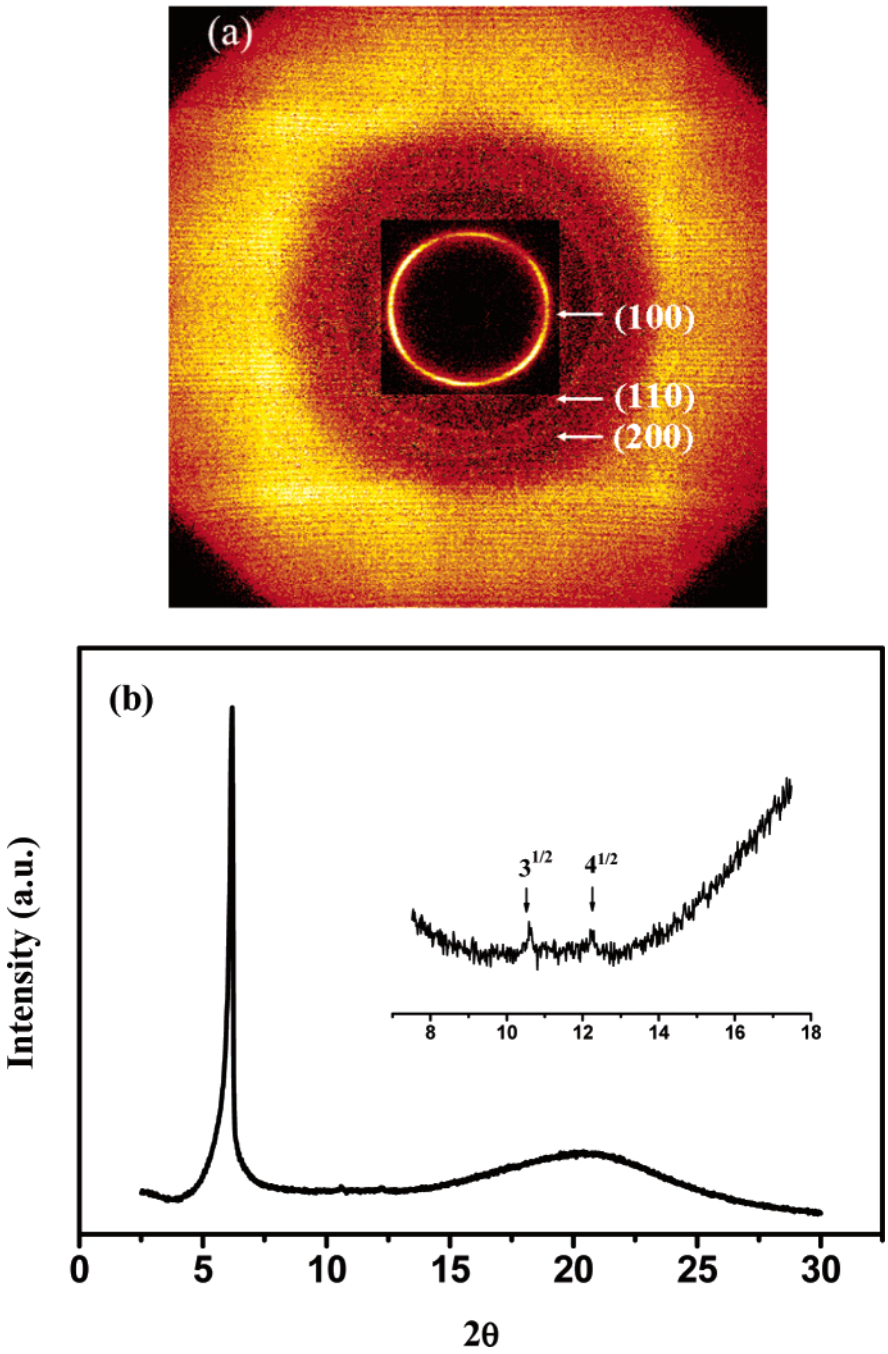

Figure 9. Two-dimensional wide-angle X-ray diffraction fiber pattern of the copolymer in which the molar fraction of MPCS in feed is 0.10 (a) and the corresponding one-dimensional wide-angle X-ray diffraction powder patterns (b).

as PBCS, and the *d* spacing kept unchanged regardless of the variations in the copolymer composition.

As has indicated in the Introduction, incorporation of nonmesogenic vinyl monomer such as St and MMA exceeding a certain amount into PMPCS backbone would cause a collapse of the "jacket effect" and destabilize the liquid crystallinity of copolymers.[59] However, all the copolymers based on MPCS and nonmesogenic BCS are able to form rather stable mesophase regardless of the composition. For the copolymers with high MPCS content, the existence of mesophase is understandable since the irregularity induced by BCS is not marked, and the copolymer main chain is still able to take extended conformation, which is a prerequisite to ordered packing for MJLCPs. Although BCS is not liquid crystalline by itself, its homopolymer does form hexagonal columnar phase.[31] The reason is that the macromolecules can act as building blocks of mesophase as a whole through the interaction of polyethylene main chain and 2,5-bis(*n*-butoxycarbonyl)phenyl side groups. As a result, it is also reasonable that the copolymers with high BCS content are liquid crystalline because MPCS as an impurity in this case has not significantly influenced the ordered packing of the copolymer in a similar way to PBCS. It is interesting to ask why the mesophase is formed in the copolymers with comparable quantity of MPCS and BCS. A possible explanation is that since both PMPCS and PBCS are ready to take cylindrical conformations,[29−31] though with slightly different diameters, 1.82 nm for PMPCS and 1.67 nm for PBCS, the random copolymers of the two can also take cylindrical conformations and thus be able to form the mesophase. The variation in mesophase dimension might be a reflection of the interruption of the presence of BCS on the mesophase formation of PMPCS, or vice versa. This is similar to main-chain liquid crystalline random copolymers

whose bulk properties show a high sensitivity to relatively small changes in the chemical structure and proportions of the monomer components.[76]

Conclusion

In summary, random copolymers of vinyl monomers, MPCS and BCS, bearing both mesogenic and nonmesogenic substituents were designed and synthesized by free radical polymerization. The reactivity ratios of MPCS and BCS determined with extended the Kelen−Tudos linearization method implied that in the copolymerization MPCS is more reactive than BCS, but the two comonomers have a tendency of random distribution. Thermal analysis showed that all the copolymers had only single glass transition, indicating again a statistical microstructure of the main chain. Unlike the copolymers based on MPCS and other nonmesogenic St and MMA as studied previously,[59] stable mesophases were established in all the copolymers we studied without minimum concentration requirement of mesogenic MPCS. An evolution of thermotropic liquid crystalline structure from Φ_{HN} to Φ_H together with the variation in mesophase dimension (*d* spacing from 1.58 to 1.44 nm at 180 °C) was achieved by tuning the ratios of comonomers in feed. To the best of our knowledge, this is the first time that both the structure and dimension of the mesophase formed by mesogen-jacketed liquid crystal polymers are manipulated through random copolymerization with nonmesogenic monomer in the whole composition range.

Acknowledgment. The financial support from the National Natural Science Foundation of China (Grants 20274001 and 20134010) and the National Distinguished Young Scholar Fund (Grant 20325415) is gratefully acknowledged.

References and Notes

(1) Hessel, F.; Finkelmann, H. *Polym. Bull. (Berlin)* **1985**, *14*, 375−378.
(2) Keller, P.; Hardouin, F.; Mauzac, M.; Achard, M. F. *Mol. Cryst. Liq. Cryst.* **1988**, *155*, 171−178.
(3) Gray, G. W.; Hill, J. S.; Lacey, D. *Mol. Cryst. Liq. Cryst.* **1990**, *7*, 47−52.
(4) Zhou, Q. F.; Li, H. M.; Feng, X. D. *Macromolecules* **1987**, *20*, 233−234.
(5) Hardouin, F.; Mery, S.; Achard, M. F.; Mauzac, M.; Davidson, P.; Keller, P. *Liq. Cryst.* **1990**, *8*, 565−568.
(6) Renz, W.; Warner, M. *Phys. Rev. Lett.* **1986**, *56*, 1268−1271.
(7) Kirste, R. G.; Ohm, H. G. *Makromol. Chem., Rapid Commun.* **1985**, *6*, 179−185.
(8) Noirez, L.; Keller, P.; Cotton, J. P. *Liq. Cryst.* **1995**, *18*, 129−148.
(9) Wang, X. J.; Warner, M. *J. Phys. A: Math. Gen.* **1987**, *20*, 713−731.
(10) Noirez, L.; Pepy, G.; Keller, P.; Benguigui, L. *J. Phys. II* **1991**, *1*, 821−830.
(11) Hardouin, F.; Mery, S.; Achard, M. F.; Noirez, L.; Keller, P. *J. Phys. II* **1991**, *1*, 511−520.
(12) Hardouin, F.; Leroux, N.; Mery, S.; Noirez, L. *J. Phys. II* **1992**, *2*, 271−278.
(13) Lecommandoux, S.; Noirez, L.; Richard, H.; Achard, M. F.; Strazielle, C.; Hardouin, F. *J. Phys. II* **1996**, *6*, 225−234.
(14) Pugh, C.; Schrock, R. R. *Macromolecules* **1992**, *25*, 6593−6604.
(15) Pugh, C.; Bae, J.-Y.; Dharia, J.; Ge, J. J.; Cheng, S. Z. D. *Macromolecules* **1998**, *31*, 5188−5200.
(16) Pugh, C.; Bae, J.-Y.; Dharia, J. G.; J. J.; Cheng, S. Z. D. *Macromolecules* **1998**, *31*, 4093−4101.
(17) Pugh, C.; Shao, J.; Ge, J. J.; Cheng, S. Z. D. *Macromolecules* **1998**, *31*, 1779−1790.
(18) Kim, G. H.; Pugh, C.; Cheng, S. Z. D. *Macromolecules* **2000**, *33*, 8983−8991.
(19) Small, A. C.; Pugh, C. *Macromolecules* **2002**, *35*, 2105−2115.
(20) Arehart, S. V.; Pugh, C. *J. Am. Chem. Soc.* **1997**, *119*, 3027−3037.
(21) Lecommandoux, S.; Hardouin, F.; Dianoux, A. J. *Eur. Phys. J. B* **1998**, *5*, 79−85.
(22) Lecommandoux, S.; Noirez, L.; Achard, M. F.; Hardouin, F. *Macromolecules* **2000**, *33*, 67−72.
(23) Pugh, C.; Kiste, A. L. In *Handbook of Liquid Crystals*; Demus, D., Goodby, J., Gray, G. W., Spiess, H. W., Vill, V., Eds.; Wiley-VCH: New York, 1998; Vol. 3.
(24) Liu, Y. X.; Zhang, D.; Wan, X. H.; Zhou, Q. F. *Chin. J. Polym. Sci.* **1998**, *16*, 283−288.
(25) Tu, H. L.; Wan, X. H.; Liu, Y. X.; Chen, X. F.; Zhang, D.; Zhou, Q. F.; Shen, Z. H.; Jason, J. G.; Jin, S.; Cheng, S. Z. D. *Macromolecules* **2000**, *33*, 6315−6320.
(26) Tu, H. L.; Zhang, D.; Wan, X. H.; Zhang, H. L.; Zhou, Q. F. *Macromol. Rapid Commun.* **1999**, *20*, 549−551.
(27) Wan, X. H.; Zhang, F.; Wu, P.; Zhang, D.; Feng, X. D.; Zhou, Q. F. *Macromol. Symp.* **1995**, *96*, 207−218.
(28) Xu, G. Z.; Wu, W.; Shen, D. Y.; Hou, J.; Zhang, F.; Xu, M.; Zhou, Q. F. *Polymer* **1993**, *34*, 1818−1822.
(29) Ye, C.; Zhang, H. L.; Huang, Y.; Chen, E. Q.; Lu, Y. L.; Shen, D. Y.; Wan, X. H.; Shen, Z. H.; Cheng, S. Z. D.; Zhou, Q. F. *Macromolecules* **2004**, *37*, 7188−7196.
(30) Yin, X. Y.; Chen, E. Q.; Wan, X. H.; Zhou, Q. F. *Chin. J. Polym. Sci.* **2003**, *21*, 9−14.
(31) Yin, X. Y.; Ye, C.; Ma, X.; Chen, E. Q.; Qi, X. Y.; Duan, X. F.; Wan, X. H.; Cheng, S. Z. D. *J. Am. Chem.* Soc. **2003**, *125*, 6854−6855.
(32) Yu, Z. N.; Wan, X. H.; Zhang, H. L.; Chen, X. F.; Zhou, Q. F. *Chem. Commun.* **2003**, 974−975.
(33) Zhang, D.; Liu, Y. X.; Wan, X. H.; Zhou, Q. F. *Macromolecules* **1999**, *32*, 5183−5185.
(34) Zhang, D.; Liu, Y. X.; Wan, X. H.; Zhou, Q. F. *Macromolecules* **1999**, *32*, 4494−4496.
(35) Zhang, D.; Zhou, Q. F.; Ma, Y. G.; Wang, X. J.; Wan, X. H.; Feng, X. D. *Liq. Cryst.* **1997**, *23*, 357−363.
(36) Zhang, H. L.; Yu, Z. N.; Wan, X. H.; Zhou, Q. F.; Woo, E. M. *Polymer* **2002**, *43*, 2357−2361.
(37) Zhou, Q. F.; Wan, X. H.; Zhu, X. L.; Zhang, F.; Feng, X. D. *Mol. Cryst. Liq. Cryst.* **1993**, *231*, 107−117.
(38) Zhou, Q. F.; Zhu, X. L.; Wan, X. H. *Macromolecules* **1989**, *22*, 491−493.
(39) Percec, V.; Pugh, C. In *Side Chain Liquid Crystal Polymers*; McArdle, C. B., Ed.; Chapman and Hall: New York, 1989.
(40) In the previous paper, the same monomer is named as di(4-butyl) vinylterephthalate (DBVT). Since both 2,5-bis[(4-methoxyphenyl)-oxycarbonyl]styrene (MPCS) and DBVT can be considered as substituted styrene monomers, 2,5-di(*n*-butoxycarbonyl)styrene (BCS) is used for the monomer in the present paper.
(41) Percec, V.; Tsuda, Y. *Macromolecules* **1990**, *23*, 5−12.
(42) Percec, V.; Tsuda, Y. *Macromolecules* **1990**, *23*, 3509−3520.
(43) Percec, V.; Tsuda, Y. *Polymer* **1991**, *32*, 673−681.
(44) Percec, V.; Yourd, R. *Macromolecules* **1989**, *22*, 524−537.
(45) Engel, M.; Hisgen, B.; Keller, R.; Kreuder, W.; Reck, B.; Ringsdorf, H.; Schmidt, H. W.; Tschirner, P. *Pure Appl. Chem.* **1985**, *57*, 1009−1014.
(46) Gray, G. M. In *Side Chain Liquid Crystal Polymers*; McArdle, C. B., Ed.; Chapman and Hall: New York, 1989.
(47) Percec, V.; Hahn, B. *Macromolecules* **1989**, *22*, 1588−1599.
(48) Platé, N. A.; Shibaev, V. P. *Comb-Shaped Polymers and Liquid Crystals*; Plenum Press: New York, 1987.
(49) Craig, A. A.; Imrie, C. T. *Polymer* **1997**, *38*, 4951−4957.
(50) Imrie, C. T.; Attard, G. S.; Kzrasz, F. E. *Macromolecules* **1996**, *29*, 1031−1035.
(51) Kosaka, Y.; Uryu, T. *Macromolecules* **1995**, *28*, 870−875.
(52) Kosaka, Y.; Uryu, T. *Macromolecules* **1995**, *28*, 8295−8301.
(53) Laus, M.; Bignozzi, M. C.; Ahgeloni, A. S.; Galli, G.; Chiellini, E. *Macromolecules* **1993**, *26*, 3999−4005.
(54) Percec, V.; Hahn, B.; Ebert, M.; Wendorff, J. H. *Macromolecules* **1990**, *23*, 2092−2095.
(55) Percec, V.; Lee, M. *Macromolecules* **1991**, *24*, 4963−4971.
(56) Percec, V.; Tomazos, D. *Macromolecules* **1989**, *22*, 1512−1514.
(57) Percec, V.; Tomazos, D. *Polymer* **1989**, *30*, 2124−2129.
(58) Percec, V.; Tsuda, Y. *Polymer* **1991**, *32*, 661−672.
(59) Zhao, Y. F.; Yi, Y.; Fan, X. H.; Chen, X. F.; Wan, X. H.; Zhou, Q. F. *J. Polym. Sci., Part A* **2005**, *43*, 2666−2674.
(60) Allegra, G.; Meille, S. V. *Macromolecules* **2004**, *37*, 3487−3496.
(61) Ganicz, T.; Stanczyk, W. A. *Prog. Polym. Sci.* **2003**, *28*, 303−329.
(62) Molengerg, A.; Moller, M.; Sautter, E. *Prog. Polym. Sci.* **1997**, *22*, 1133−1144.
(63) Out, G.; Turetskii, A.; Moller, M.; Oelfin, D. *Macromolecules* **1994**, *27*, 3310−3318.
(64) Out, G.; Turetskii, A.; Moller, M.; Oelfin, D. *Macromolecules* **1995**, *28*, 596−603.
(65) Harwood, H. J.; Baikowitz, H.; Trommer, H. F. *Polym. Prepr.* **1963**, *4*, 133−141.
(66) Coskun, M.; Ilter, Z. *J. Polym. Sci., Part A* **2002**, *40*, 1184−1191.
(67) Ilter, Z.; Soykan, C.; Koca, M. *J. Polym. Sci., Part A* **2003**, *41*, 2996−3005.

(68) Mayo, E. R.; Lewis, E. M. *J. Am. Chem. Soc.* **1944**, *66*, 1594−1601.
(69) Stanek, L. G.; Heilmann, S. M.; Gleason, V. B. *J. Polym. Sci., Part A* **2003**, *41*, 3027−3037.
(70) Zhang, H. W.; Hong, K.; Jablonsky, M.; Mays, J. W. *Chem. Commun.* **2003**, 1356−1357.
(71) Ziaee, F.; Nekoomanesh, M. *Polymer* **1998**, *39*, 203−207.
(72) Elias, H. G. *Macromolecules*; Plenum: New York, 1977; Vol. 2.
(73) Gopalan, P.; Ober, C. K. *Macromolecules* **2001**, *34*, 5120−5124.
(74) Wunderlich, B. *Thermal Analysis*; Academic Press: Boston, 1990.
(75) Percec, V.; Lee, M. J. *Mater. Chem.* **1992**, *2*, 617−623.
(76) Blackwell, J.; Biswas, A. In *Developments in Oriented Polymers-2*; Ward, I. M., Ed.; Elsevier: Barking, UK, 1987.

MA0608774